

# Balloon-Borne Investigation of Zenith Angle Dependence of Cosmic Ray Showers

Alynie Walter<sup>1</sup>, Alisha Wiedmeier<sup>2</sup>, Melissa Graham<sup>2</sup>, Judy Panmany<sup>2</sup>, Claire Weinzierl<sup>2</sup>, Erick Agrimson<sup>3</sup>  
*St. Catherine University, St. Paul, Minnesota, 55105*

Gordon McIntosh<sup>4</sup>  
*University of Minnesota-Morris, Morris, Minnesota 56267*

and  
James Flaten<sup>5</sup>  
*MN Space Grant/University of Minnesota – Twin Cities, Minneapolis, Minnesota, 55455*

**Galactic Cosmic Rays are high-energy particles from stars or remnants of a supernova. These particles impinge upon the Earth's atmosphere in the form of positively-charged particles – protons. Protons interact with atmospheric nuclei to produce a cascade of high-energy secondary particles known as a Galactic Cosmic Ray Shower. Post-collision secondary shower details depend on altitude, latitude, solar activity, and air pressure. The Regener-Pfotzer (R-P) maximum, which occurs between 15,000 m and 25,000 m, is the altitude where the maximum number of detections is measured with a Geiger-Müller detector (often called a Geiger counter). In order to quantify cosmic ray events, a payload was flown on stratospheric balloon flights containing four Geiger counters in a vertical cross configuration measuring omnidirectional cosmic ray levels from a single Geiger counter as well as vertical and horizontal coincidences between pairs of Geiger counters. Analyzed data showed the R-P maximum occurring at different altitudes for omnidirectional measurements, vertical coincidences, and horizontal coincidences, consistent with previous research.**

## Nomenclature

HAB = High-Altitude Balloon  
G-M = Geiger-Müller  
R-P = Regener-Pfotzer  
GCRS = Galactic Cosmic Ray Shower

## I. Introduction

Cosmic radiation was discovered by Victor Hess in a series of balloon flights up to an altitude of 5 km between 1911 and 1913. This discovery ultimately led to Hess receiving the Nobel prize in 1936<sup>1</sup>. This work was followed up with the first stratospheric manned balloon flight by Piccard and Cosyns in 1933, reaching an altitude of 16 km and recording stratospheric radiation as they flew in a pressurized capsule<sup>2</sup> shown in Figure 1. Peters<sup>3</sup> provides an extensive review of the development of cosmic ray research from the mid 1940's until the late 1950's outlining some of the early high-altitude balloon (HAB) flights looking at cosmic rays. Grieder<sup>4</sup> has written an extensive overview

---

<sup>1</sup> Alumna summer assistant 2019, St. Catherine University, 2004 Randolph Ave., St. Paul, MN, 55105.

<sup>2</sup> Undergraduate Student, St. Catherine University, 2004 Randolph Ave., St. Paul, MN, 55105.

<sup>3</sup> Associate Professor of Physics, St. Catherine University, 2004 Randolph Ave., St. Paul, MN, 55105.

<sup>4</sup> Professor of Physics, University of Minnesota, Morris, 600 East 4th St., Morris, MN, 56267.

<sup>5</sup> Associate Director of the MN Space Grant Consortium, Aerospace Engineering and Mechanics Department, University of Minnesota – Twin Cities, 110 Union St., SE, Minneapolis, MN, 55455.

of all cosmic ray research up until the turn of the 21<sup>st</sup> century listing many ground-based, HAB-based, and satellite-based measurements.



Figure 1. Stratospheric Piccard Balloon gondola at the Museum of Science and Industry in Chicago. Photo taken by E. Agrimson on 7/13/18.

Galactic Cosmic Rays are constantly impinging Earth's atmosphere, typically in the form of protons. These protons interact with atmospheric nuclei and the resulting collision creates a cascade of high-energy secondary particles called a Galactic Cosmic Ray Shower (GCRS). Details of GCRSs depend on the altitude, latitude, and solar activity (following the 11-year solar cycle for lower energies) present on the Earth<sup>4</sup>. GCRSs are the result of distant sources, such as stars or remnants of a supernova. By the time these secondary particles reach the Earth's surface, they are mostly muons. In order to detect the most-diverse range of particles, measurements must be made in situ. GCRs, as described in ref. [4] and illustrated in Figure 2, can be classified into three main components: the electromagnetic (mostly photon- electron components) driven by neutral pion decay, the hadronic component (which constitutes the core portion of the showers), and the mesonic component driven mainly by decay of pions into muons.

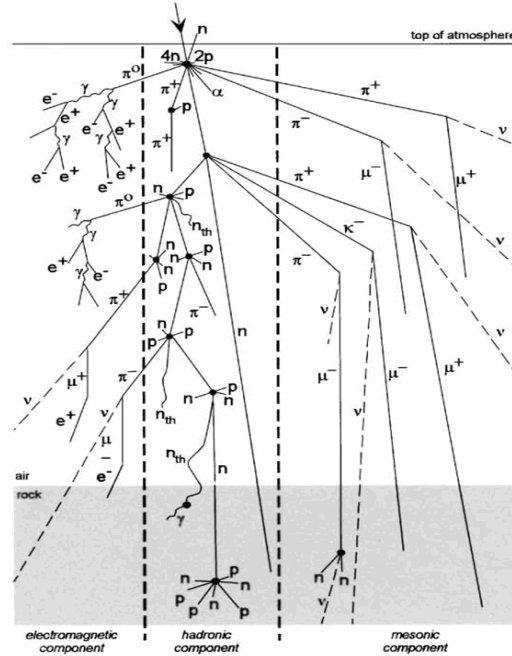


Figure 2: Components of a cosmic ray shower<sup>5</sup>.

Between 15,000 and 25,000 m in altitude lies the Regener-Pfotzer (R-P) Maximum<sup>6-7</sup>. This maximum is the altitude at which the largest number of counts per unit time are measured with a Geiger-Müller (G-M) detector (also called a Geiger counter). The unit of measure used in data collection is counts per unit time, where each count is the detection of a single high-energy particle or cascade. Depending on factors such as the altitude, solar activity, pressure, temperature, density, and geomagnetic latitude, the R-P Maxima can occur at different altitudes<sup>8-10</sup>. The directional intensity (I) of the R-P maximum can be described by  $I(\theta, \varphi) = \frac{dN}{dA dt d\Omega}$  where N is the number of particles, A is the detector's element area, t is time, and  $\Omega$  is solid angle<sup>4</sup>. Furthermore, the detection of a cosmic ray "coincidence" depends on the solid angle of one detector being superimposed on the solid angle of a second detector so that a single cosmic ray, following a straight line, can pass through and trigger both detectors, being stopped/deflected by neither. The solid angle<sup>11</sup> of a vertical coincidence is the intersection between two detectors mounted one directly above the other as shown in Figure 3 below, where  $\Omega = \int \frac{\cos\alpha}{r^2} dA$ . Here  $\Omega$  represents the solid angle in steradians subtended by the detector and r is the distance from the source and the surface element dA;  $\alpha$  is the angle between the normal to surface element and the source direction. For a point source located along the axis of a cylindrical detector, the solid angle is given by  $\Omega = 2\pi \left(1 - \frac{d}{\sqrt{d^2+a^2}}\right)$ , where d is the source-to-detector distance and a is the detector radius. In the limit where  $d \gg a$ , the solid angle can be approximated as  $\Omega \approx \frac{\pi a^2}{d^2}$ . The solid collection angle based on our payload box separation distance for the two Aware Electronics RM-80 (Roentgen Monitor) G-M detectors was calculated to be 0.275 steradians. The detection of a particle in both detectors simultaneously is defined as coincidence. These coincidences provide insight into the direction of the particle's directly of travel. Horizontal coincidence occurs similarly to vertical coincidence; however, the two RM-80 G-M detectors are rotated 90 degrees and separated horizontally by the same distance as the pair of vertical sensors (see Figure 3). Of note, the experimental design was motivated by a previous payload that contained just one pair of stacked RM-80 detectors which could be tipped by a servo-motor with respect to vertical during the flight, to measure coincidences at varying angles<sup>12</sup>.

Vertical coincidence occurs when two detectors are aligned as shown in Figure 3. A vertical coincidence is detected when a cosmic ray follows a path within in innermost cone, passing through and triggering both detectors essentially simultaneously. The RM-80 model from Aware Electronics was used to measure the coincidence of the GCRS. Note that the RM-80 is a "pancake" shaped G-M tube. The pancake shape assists in maximizing the detected cosmic ray flux in the vertical direction and minimizes the flux detected from other directions.

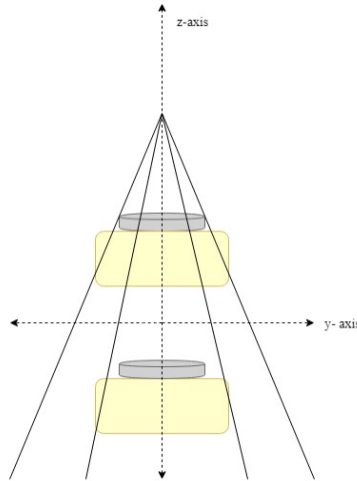


Figure 3. Showing solid angle detection of charged event in two separated pancake type detectors – diagram based on Figure 1 from ref. [13].

## II. Collection of Cosmic Ray data

The "Quad box", as we call this particular payload, contains four RM-80 (Radiation Monitor) Geiger counters configured in a "bunk bed" design (see Figure 4 for schematic and Figure 5 for picture of the Quad box), a heater

circuit, two pressure sensors, and a GPS. Two Arduino Mega microcontrollers were utilized to control various portions of the payload. This payload was flown on three occasions, 6/7/19 (Flight  $\alpha$ ), 6/13/19 (Flight  $\beta$ ), and 7/27/19 (Flight  $\gamma$ ), as part of the overall stack.

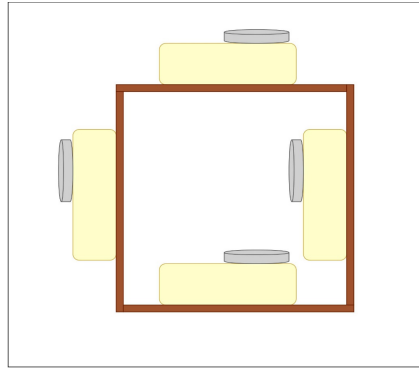


Figure 4. Side view of the four RM-80 Geiger counters in the Quad Box



Figure 5. Layout of the Quad box just before flight.

The “bunk bed” design was implemented to best-measure the vertical and horizontal coincidences that occur when the detectors are aligned at a specified angle. The detectors were intentionally separated in this configuration so the detector pairs were able to measure a narrower view and the coincidence readings were, therefore, more closely aligned with vertical and horizontal axes. This was a change from our 2018 G-M work<sup>12</sup> where the detectors were in very close proximity to each other, therefore resulting in a wider field of view.

In addition, an omnidirectional R-P maximum was measured using an RM-60, which was part of a separate payload on the same stack – this was due to payload mass limitations. The RM-60 uses a cylindrical tube rather than the pancake type tube used in the RM-80 detectors. For this reason, it is able to more-evenly collect events from all directions and thus is used as the omnidirectional measurement standard.

### III. Results

The three flights ( $\alpha$ ,  $\beta$ , and  $\gamma$ ) documented that the R-P maximum of the omnidirectional counts, the vertical coincidences, and the horizontal coincidences occurred at different altitudes. Due to a malfunction of a Geiger counter, figures were not able to be constructed for Flight  $\alpha$ . For Flights  $\beta$  and  $\gamma$  data analysis similar to ref. [14] was done. Figures 6-11 were each fitted with a third-order polynomial. Of note, Figure 8 and Figure 9 have a larger y axis due to the omnidirectional G-M tube obtaining counts from all directions as compared to data collected with the pancake G-M tubes (see Figures 6, 7, 10, and 11) which more effectively select particles from one direction.

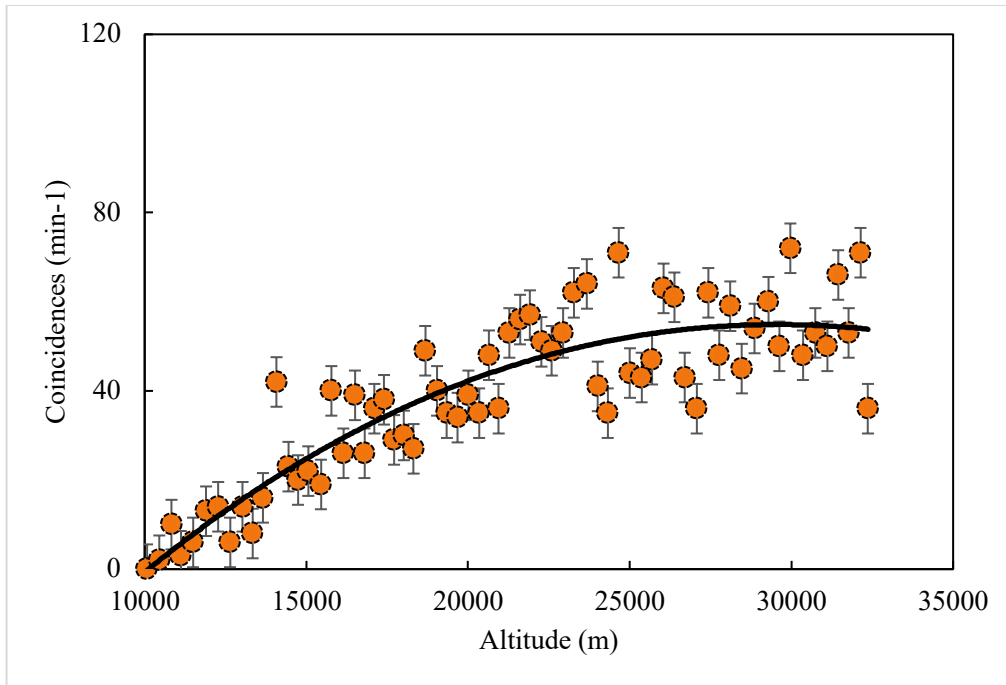


Figure 6. Flight  $\beta$ : Altitude vs. Horizontal Coincidences. R-P max at 29,500 m.

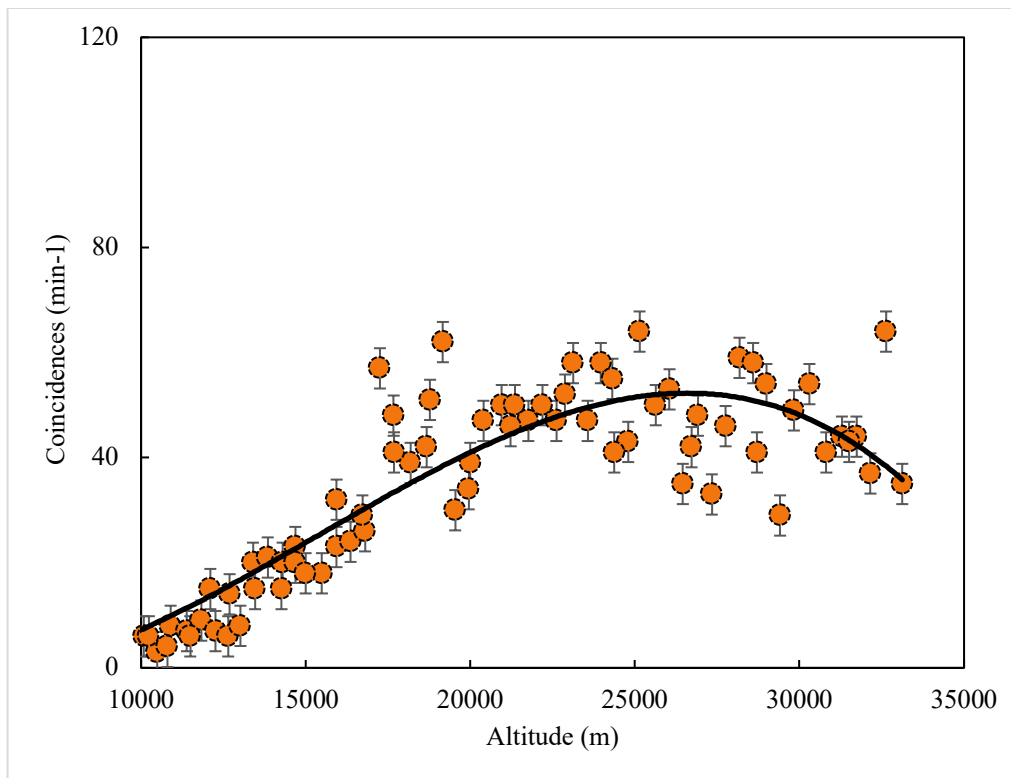


Figure 7. Flight  $\gamma$ : Altitude vs Horizontal Coincidences. R-P max at 26,600 m.

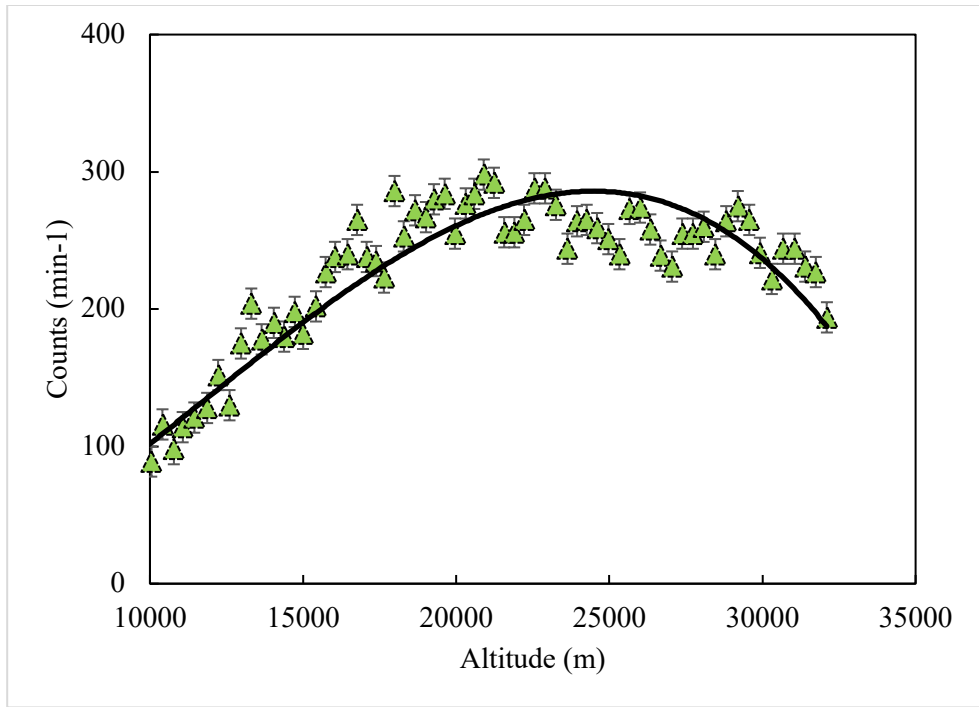


Figure 8. Flight  $\beta$ : Altitude vs. Omnidirectional Counts. R-P max at 24,500 m.

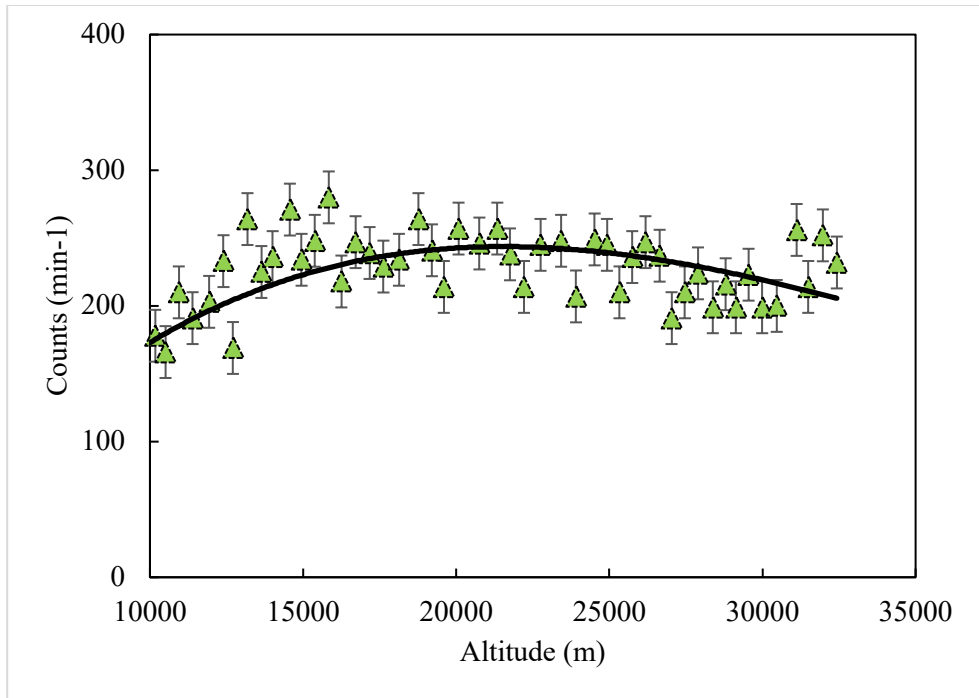


Figure 9. Flight  $\gamma$ : Altitude vs Omnidirectional Counts. R-P max at 21,400 m.

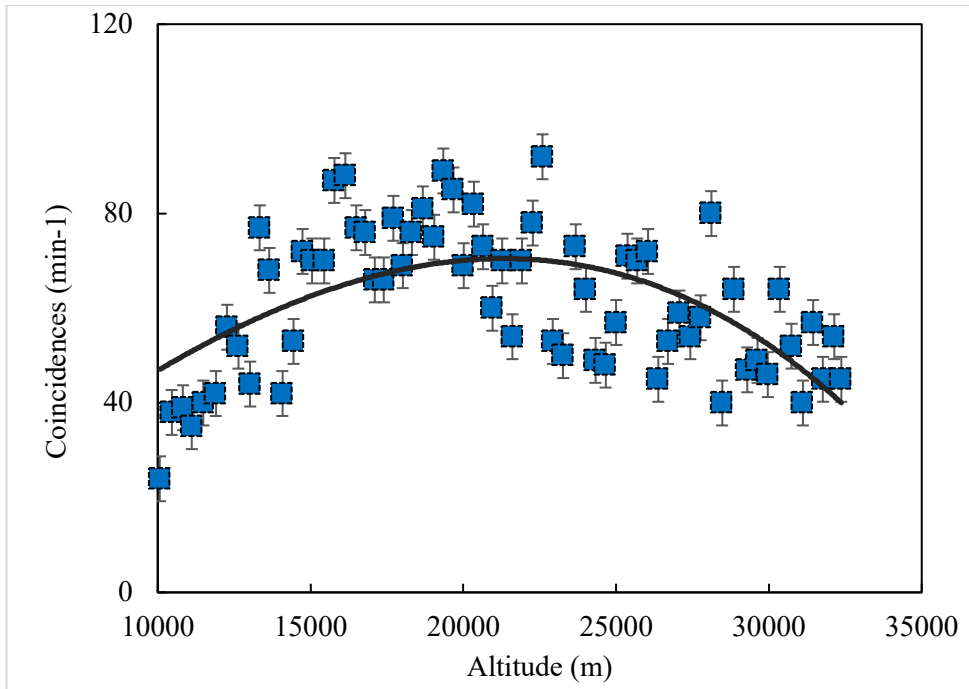


Figure 10. Flight  $\beta$ : Altitude vs. Vertical Coincidences. R-P max at 21,300 m.

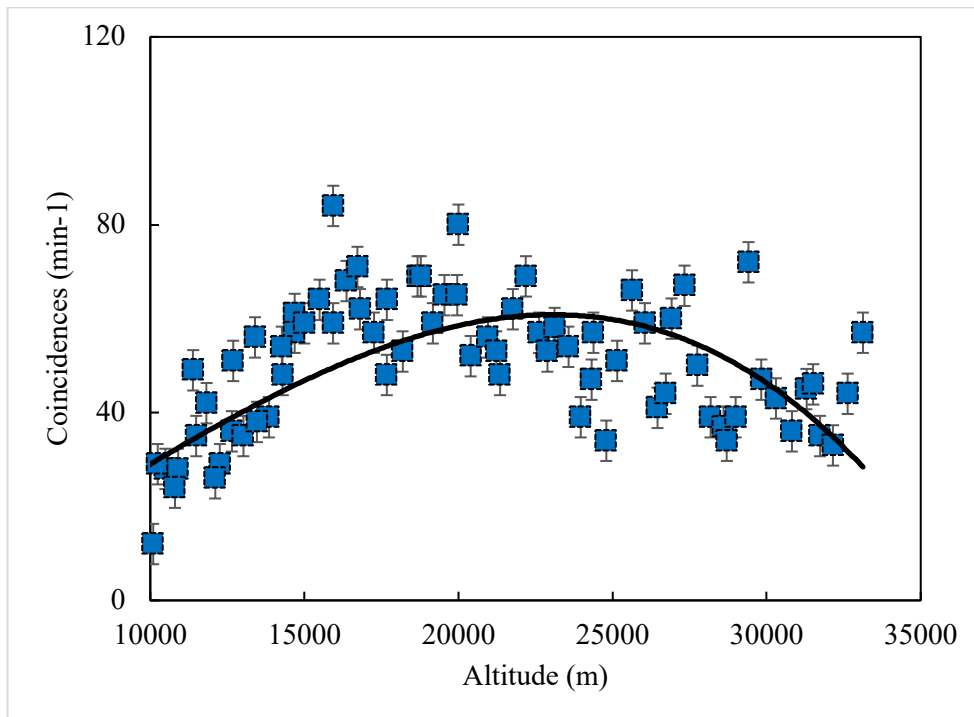


Figure 11. Flight  $\gamma$ : Altitude vs. Vertical Coincidences. R-P max at 23,000 m.

Table 1 shows that the horizontal coincidence R-P maximum altitude ranged from 25,300 m to 29,500 m whereas the omnidirectional R-P maximum occurred at a lower altitude on each flight, ranging from 21,400 m to 24,500 m. Due to a malfunction of one Geiger counter in the vertical coincidence pair during Flight  $\alpha$ , it was not possible to

accurately obtain a vertical coincidence R-P maximum from that flight; this is noted in Table 1. The horizontal coincidence R-P maxima resulted in the highest altitude for all three flights, where the vertical R-P coincidence maxima were, on average, the lowest. Vertical and horizontal maxima occur at differing altitudes solely based on the dispersion of GCRS. This concept comes from the argument in ref. [10], particles tend to travel more along the azimuth, as the largest momentum tends to be in this direction. This differs as compared to the horizontal direction which would tend to be more due to shower/collisional effects.

**Table 1: Zenith angle R-P maximum determination. Uncertainty for all values is  $\pm 1,000$  m.**

R-P Max	<i>Flight <math>\alpha</math>, (3<sup>rd</sup> order poly fit)</i> <i>m</i>	<i>Flight <math>\beta</math>, (3<sup>rd</sup> order poly fit)</i> <i>m</i>	<i>Flight <math>\gamma</math>, (3<sup>rd</sup> order poly fit)</i> <i>m</i>
Horizontal	25,300	29,500	26,600
Omnidirectional	24,500	24,500	21,400
Vertical	NA	21,300	23,000

Figures 11-13 show one-minute averages for Flights  $\alpha$ ,  $\beta$ , and  $\gamma$  from data collected with the vertically-oriented pair of RM-80s as well as the horizontally-oriented pair RM-80s. Notice that the vertical-coincidence R-P maximum occurs at a lower altitude than the horizontal-coincidence R-P maximum in the flights where both were able to be determined. This data supports the argument in ref. [10] that particles tend to travel more along the azimuth, as compared to the horizontal which would tend to be more due to shower/collisional effects. This is also supported by the significantly-larger number of vertical coincidences than horizontal coincidences below 20,000 m. The vertical coincidence counts typically have at least 70 coincidences per minute in the vertical direction as compared to roughly 60 in the horizontal direction within the R-P maximum region. In addition to this, the data shows that the vertical coincidences maintain a large number of counts per minute lower in altitude, as compared to horizontal coincidences. The horizontal red dashed lines at 15,000 m and 25,000 m on the graphs indicate the typical referenced altitude range of the (omnidirectional) R-P maximum <sup>4, 6-7</sup>.



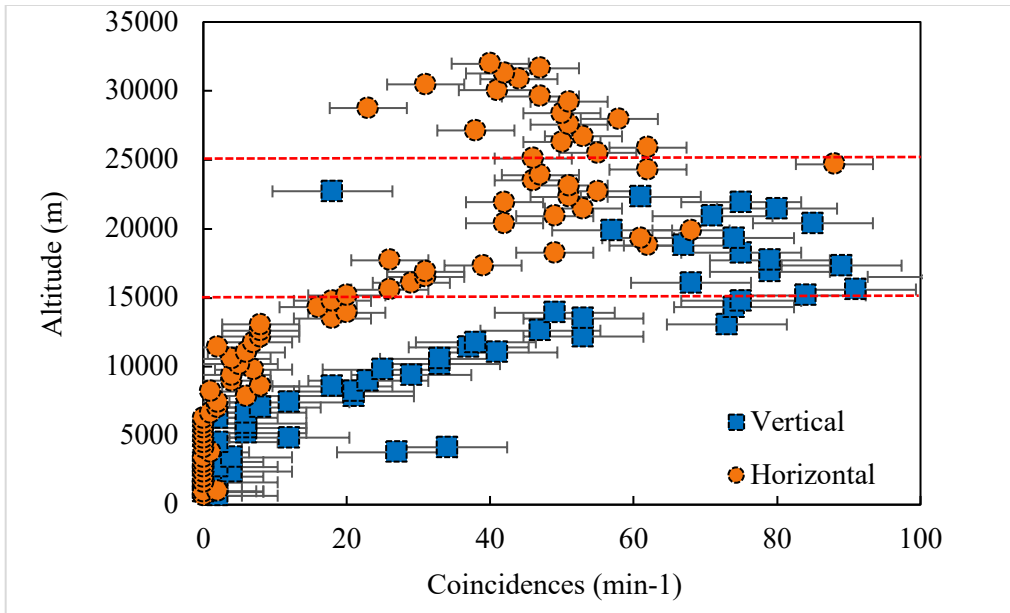


Figure 12. Vertical and Horizontal Coincidences vs. Altitude for Flight  $\alpha$ . One Geiger counter in the vertical-coincidence pair malfunctioned during this flight so the vertical-coincidence R-P maximum altitude could not be determined accurately.

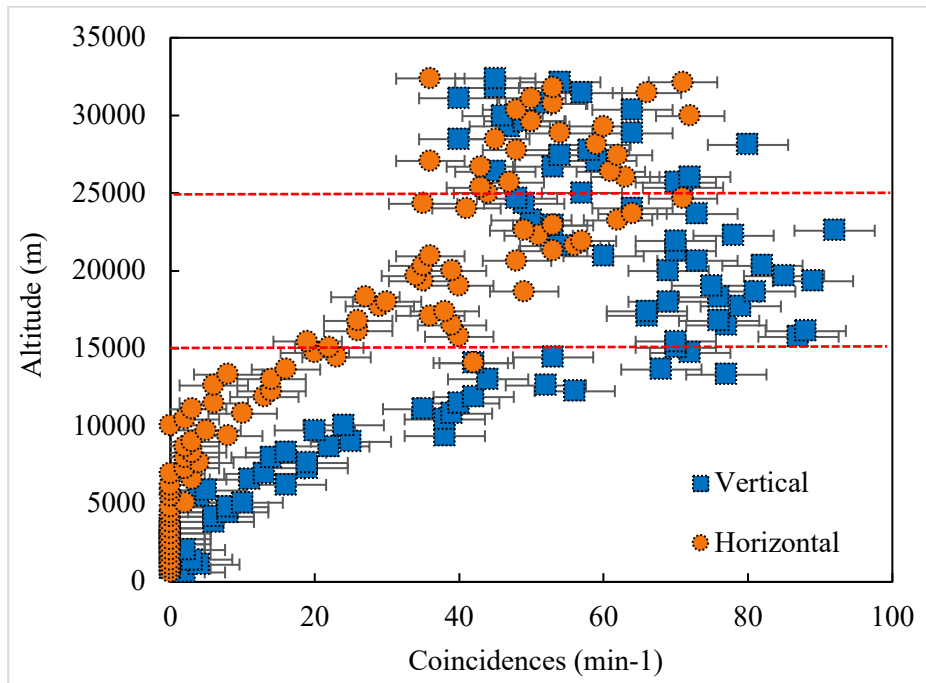


Figure 13. Vertical and Horizontal Coincidences vs. Altitude for Flight  $\beta$ .

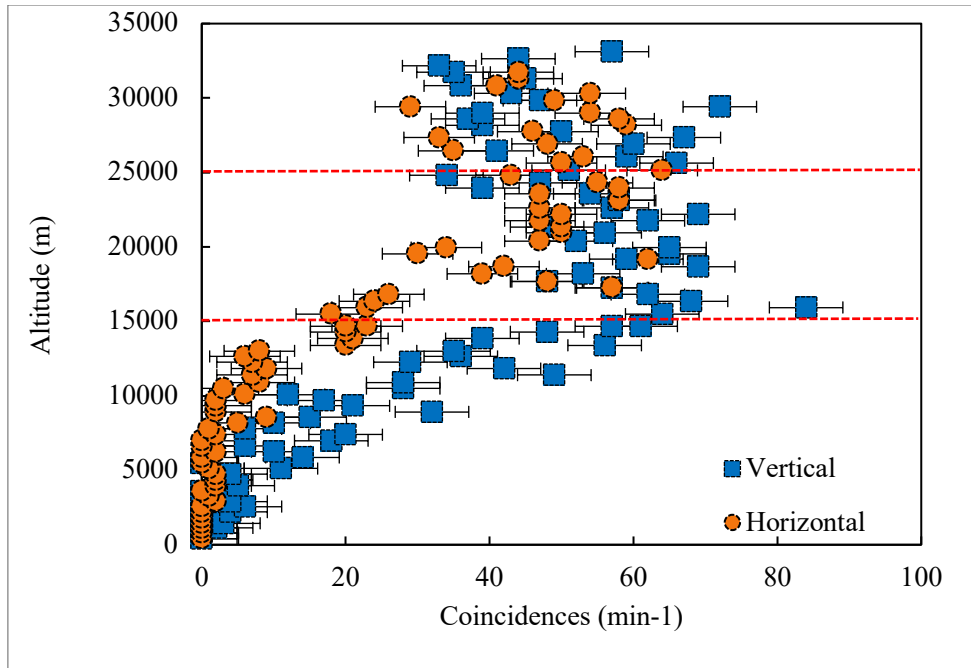


Figure 14. Vertical and Horizontal Coincidences vs. Altitude for Flight  $\gamma$ .

#### IV. Summary

Our results show that the R-P maximum occurs at a lower altitude for vertical-coincidences than for horizontal-coincidences. For Flights  $\beta$  and  $\gamma$  (the two flights that had a full set of functioning Geiger counters throughout the flight), the horizontal coincidence R-P maximum was higher than the vertical coincidence R-P maximum by 8,200 m for Flight  $\beta$  and 3,600 m higher for Flight  $\gamma$ . Both of these results are well outside the relative differences within the R-P max. altitudes. The pair of vertically-oriented G-M pancake detectors recorded more coincidence events occurring at lower altitudes. For example, almost zero coincidence counts occur at ground level in the horizontal direction, but as many as 5 coincidence counts per minute occur at ground level in the vertical direction. At 15,000 m there were typically about 20 horizontal coincidence counts per min. Vertical coincidence counts per min ranged from 60 to 80, at least three times as many counts as the horizontal, at 15,000 m.

In addition, at 15,000 m altitude there were typically about 20 horizontal coincidence counts per minute but at the same altitude the vertical coincidence counts per minute ranges from 60 to 80 – at least three times as many counts. The omnidirectional counts R-P max always occurred at a lower altitude as compared to the corresponding horizontal coincidence R-P max. On Flight  $\alpha$  it was 0.8 km lower. On Flight  $\beta$  it was 5,000 m lower. And on Flight  $\gamma$  it was 5,200 m lower. Even an estimated vertical coincidence R-P max from Flight  $\alpha$  was outside of the uncertainty in the measurements, and as such all of these are significant results.

We also recorded triple and quadruple coincidences for the three flights, though additional analysis needs to be done in relation to those measurements. Coincidences in more than two non-aligned Geiger counters is due to counters being triggered by different particles from a single shower. Analysis of that additional data may help us estimate what fraction of horizontal coincidences, for example, are actually due to vertical showers rather than horizontally-moving single high-energy particles.

#### Acknowledgments

We would like to thank the Minnesota Space Grant Consortium for financial support of ballooning activities since 2007. Funding was also provided in the summer of 2019 by the St. Catherine University Summer Scholars Program. We also would like to thank the Morris Academic Partnership and the University of Minnesota, Morris.

## References

- [1] Hess, V. F. The Nobel Prize in Physics 1936.  
URL: <https://www.nobelprize.org/prizes/physics/1936/hess/biographical/> [Retrieved March 30, 2018]
- [2] Piccard, A. and Cosyns, M. *Comptes rendus de l'academie de mathem*, 195 No. 1, 1932, p 604.
- [3] Peters, B. "Progress in Cosmic Ray Research since 1947" *Journal of Geophys. Research* 64, No. 2 1959.  
doi: 10.1029/JZ064i002p00155
- [4] Grieder, P. *Cosmic Rays at Earth* 2001.
- [5] URL: <https://malagabay.wordpress.com/2014/07/27/atmospheric-science-burying-beals-barometer/>  
[Retrieved March 30, 2018]
- [6] Regener, E., "New Results in Cosmic Ray Measurements," *Nature*, Vol. 132, 1933, pp. 696-698.  
doi: 10.1038/132696a0
- [7] Carlson, P., & Watson, A. A. (2014, November 18). *Erich Regener and the maximum in ionisation of the atmosphere*. In *History of Geophysics and Space Science*. [Retrieved March 30, 2018]  
URL: <https://arxiv.org/ftp/arxiv/papers/1411/1411.6217.pdf>  
doi: 10.5194/hgss-5-175-2014
- [8] Bhattacharyya, A. et al., "Variations of  $\gamma$ -Ray and particle Fluxes at the Sea Level during the Total Solar Eclipse of 24 October, 1995," *Astrophys. Space Science*, Vol. 250, 1997, pp. 313-326.  
doi: 10.1023/A:100040822978
- [9] Harrison, R., Nicoll, K., & Aplin, K., "Vertical profile measurements of lower troposphere ionization," *Journal of Atmospheric and Solar-Terrestrial Physics*, Vol. 119, 2014, pp. 203-210. 2014.  
doi: 10.1016/j.jastp.2014.08.006
- [10] Mishev, A. "Short- and Medium- Term Induced Ionization in the Earth Atmosphere by Galactic and Solar Cosmic Rays," *International Journal of Atmospheric Sciences*. 2013.  
doi: 10.1155/2013/184508
- [11] Knoll, G. *Radiation Detection and Measurement* 4<sup>th</sup> Edition 2010.
- [12] Walter, A., Wiedmeier, A., Montenegro Cortez, V., Ezenagu, N., Agrimson, E., Smith, K., McIntosh, G., and Flaten, J. "Building a Balloon Borne Apparatus to Measure Zenith Angle Dependence of Cosmic Ray Showers in the Stratosphere" in *the Proceedings of the 9<sup>th</sup> Annual Academic High Altitude Conference*, Omaha, NE, USA, 2018.
- [13] El-Khatib, A., Badawi, M., Abd-Elzaher M., & Thabet A "Calculation of the Peak Efficiency for NaI (Tl) Gamma Ray Detector Using the Effective Solid Angle Method," *Journal of Advanced Research in Physics*. 2012.
- [14] Taylor, L., McIntosh, G., Swanson, A., Agrimson, E. and Smith, K., poster in *the Proceedings of the 8<sup>th</sup> Annual Academic High Altitude Conference*, University of Minnesota, Minneapolis, MN, USA, 2017.  
URL: <https://www.iastatedigitalpress.com/ahac/article/id/9756/>